Catalysis Today 176 (2011) 41–47

Contents lists available at ScienceDirect

Catalysis Today

journal homepage: www.elsevier.com/locate/cattod

Reduction of oxygen at the interface M|solid oxide electrolyte (M = Pt, Ag and Au, solid oxide electrolyte = YSZ and GDC). Autocatalysis or artifact?

Andrzej Raźniak*, Magdalena Dudek, Piotr Tomczyk

Faculty of Energy and Fuels, AGH – University of Science and Technology, al. A. Mickiewicza 30, 30-059 Krakow, Poland

ARTICLE INFO

Article history:
Received 30 September 2010
Received in revised form 18 April 2011
Accepted 19 April 2011
Available online 17 May 2011

Keywords:
Oxygen reduction
8YSZ
20GDC
Metal migration
Three phase boundary

ABSTRACT

The process of oxygen reduction at an interface metallic microelectrode solid oxide electrolyte was investigated at 700 °C under various oxygen partial pressures. In these experimental conditions, an increase of absolute current was observed when the electrodes made of Pt, Ag and Au were polarized with negatives overpotential down to −0.3 V. Such an unusual behaviour was explained by the increase of the three-phase boundary length due to the deposition and subsequent reduction of metal oxides in the vicinity of Pt and Ag electrodes. However, in the case of Au electrode, no pattern of migrated metal was observed around the electrode. In this case, the occurrence of autocatalytic electrode reaction is suggested to explain the phenomenon.

1. Introduction

The first investigations of the oxygen electrode reaction (OER) on solid oxide electrolytes were performed over a hundred years ago and regarded problems relevant to electric lighting. Then, the OER and solid oxide electrolytes attracted renewed attention when an idea of solid oxide fuel cell (SOFC) gave a chance to build a power generator, almost perfectly suitable to the decentralized energy system [1–3]. As many as over a thousand of articles pertinent to SOFC cathodic process and cathode materials have been published in major scientific journals since 1980.

The extensive works on the OER mechanism were firstly performed with porous platinum electrodes and yttria stabilized zirconia (YSZ) electrolyte. Then, the studies were extended to electrodes made of other noble metals and mixed-conducting materials; the latter ones were introduced to improve performance of SOFC due to an extension of cathodic reaction zone. Now, the experiments are often carried out with electrolytes and electrodes, which can be effectively employed in an intermediate temperature solid oxide fuel cell (ITSOFC), i.e. whose characteristics are more favourable for operation at the temperatures in the range of 700–800 °C.

Today, despite numerous works and a long time of research, the OER at Pt and other noble metals is still actively studied because it constitutes a useful basis on which the understanding of all SOFC cathodes can be built. Generally, these experiments can be split into two fundamentally different schools of reasoning. The first one, rooted in the well-established tradition of classical electrochemical kinetics, focused on the observation that the oxygen electrodes at solid oxide electrolytes tend to obey Tafel kinetics at moderate to high overpotential [4–9]. Therefore, these data were typically analyzed in terms of specific rate-limiting steps occurring at the interface. The second school concentrated on the results obtained by electrochemical impedance spectroscopy (EIS), nevertheless, when these spectra were simulated by an equivalent RC circuit, the model was frequently incoherent with physical and chemical properties of an interface [10–12]. Hence, another explanation of these data was sought, which had to take into consideration the complexity of faradaic process, with the possibility that more than one rate-limiting reaction step could dominate under various conditions [13–17].

The strong evidence showing that co-limited adsorption and surface diffusion play a significant role in the overall reaction

$$O_2 + 4e^- \rightarrow 2O^{2-} \quad (1)$$

was given by Mitterdorfer and Gauckler [18–20]. Despite a considerable progress made in the recent years in understanding of solid oxide fuel cell cathodes, many open questions, relevant to the OER at Pt and other noble metals, remain still open to the discussion. Obviously, additional questions regard the technologically advanced cathodes of contemporary SOFCs, which are made of MIEC composite materials.

Some hope to enlighten at least some of controversies over the OER appeared when using point and quasi-point solid electrodes

* Corresponding author. Tel.: +48 12 6173998; fax: +48 12 6174547.
E-mail address: razniak@agh.edu.pl (A. Raźniak).

0920-5861/$ – see front matter © 2011 Elsevier B.V. All rights reserved.
doi:10.1016/j.cattod.2011.04.030

because they facilitate the investigation of the charge transfer reaction, enable the properties of electrode surface and electrolyte to be scanned and the effect of ohmic drops to be reduced. Unfortunately, the use of microelectrodes appeared to be only a little helpful for clarifying the controversies but it revealed also a new unresolved issue, namely the so called nonstationary behaviour of metallic electrodes, such as hysteresis or inductive effects, which were manifested under negative and positive polarizations. Many authors reported such findings, first of all, for the Pt electrodes, although the similar behaviour was also observed for the Au, Pd and Ag electrodes [21–27]. One of the "nonstationary behaviour" indication consists in a distinct increase of the absolute current flowing through the metallic electrode located on the solid oxide electrolyte during a prolonged negative polarization. This phenomenon is somehow consistent with an improvement of cathode operation of the state-of-the-art SOFC, which is usually observed at the beginning of loading the cell [28–33].

A number of explanations for this behaviour, such as the effect of reactive intermediates on the Pt surface, passivation of the Pt surface by platinum oxides, expansion of the reaction zone along the YSZ surface and Joule heating of the sample had been subsequently rejected until Nielsen and Jacobsen [25–27] observed at SEM images the dendrite-like structure of Pt around the electrode. The SEM pictures were made for quenched samples after the experiments performed with the Pt electrode polarized with low and moderate negative overpotentials at 1000 °C. Therefore the increase of cathodic current has been unambiguously attributed to the increase of TPB (three-phase boundary) length, which grows during the formation of a dendrite-like structure, due to the migration of metal from the negatively polarized electrode.

In the present paper, we investigate the OER at the interface metal|solid oxide electrolyte using microelectrodes, with the emphasis put on the effect of prolonged polarization of the electrode and phenomenon of extension of TPB length by metal migration from the electrode. The experiments were performed at 700 °C, which corresponds to the operational temperature of IT-SOFC. Two of electrolytes were used in the studies: yttria stabilized zirconia (8YSZ) and gadolina doped ceria (20GDC), the electrodes were made of Pt, Ag and Au. Both these electrolytes, 8YSZ and 20GDC, are high oxygen ion conductors with the same ion transport mechanism through oxygen deficiency. We performed the comparative experiments for these two electrolytes to justify that the mechanism of ion conductance had a dominant effect on the phenomena reported in this work. The main aims of the work are to explain mechanism of metal migration to the vicinity of electrode and answer the question if only this phenomenon is exclusively responsible for the "nonstationary behaviour" of the systems investigated.

2. Experimental

The experimental set up and procedures of electrochemical measurements were described elsewhere [34]. The electrolytes were sintered from powders of ZrO_2 + 8 mol% Y_2O_3 (8YSZ) and CeO_2 + 10 mol% Gd_2O_3 (20GDC), which were disc shaped of 10 mm diameter and 3 mm thickness. During the measurements, two microelectrodes were located on opposite sides of the electrolyte disc; these electrodes were used alternatively as a working and reference electrode. The electrodes and disc were assembled inside the alumina holder and gripped together due to the action of springs with the force of about 0.5 N. A counter electrode, in the form of platinum ring made from a wire of diameter 0.5 mm, was located in a furrow grooved around the side wall of the disc. The experiments were performed in a stream of O_2 + Ar mixture at 50 ml/min flow rate. An AUTOLAB electrochemical station was used in these measurements.

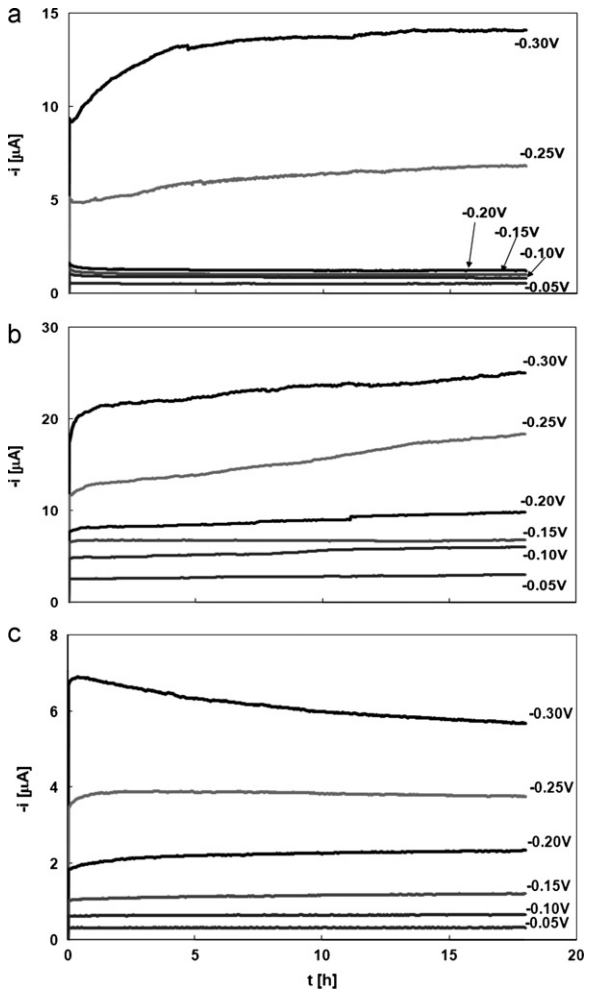

Fig. 1. Family of chronoamperometric curves recorded at point electrodes: (a) Pt, (b) Ag, (c) Au, in contact with 20GDC electrolyte (overpotentials are given over the respective curves, atmosphere $0.1O_2$ + 0.9Ar, 700 °C).

Before and after the electrochemical experiments, the surfaces of the Au, Pt and Ag quasi-point electrodes as well as 8YSZ and 20GDC pellets were examined by means of a scanning electron microscope (SEM/EDX), X-ray Photoelectron Spectroscopy/Electron Spectroscopy for Chemical Analysis (XPS/ESCA) and Atomic Force Microscopy (AFM). The SEM microphotographs, XPS/ESCA and AFM analysis were made for the quenched samples prepared in a set-up similar to the electrochemical cell. The only differences between these set-ups were such that in the former the working electrode was polarized in a two electrode system and a large porous Pt plaque was used as a common reference and counter electrode. During the preparation of the sample, the working microelectrode was polarized several hours with overpotential of −0.5 V, then the system was cooled down to the room temperature in 2–3 h. Also during the cooling, the overpotential of the working electrode was held at −0.5 V as long as possible. Additional samples of electrolytes with unpolarized electrodes were also prepared in analogous conditions for the examination with the SEM/EDX, XPS/ESCA and AFM techniques.

3. Results and discussion

Typical dependences of the currents flowing through the electrode at different negative step-like polarizations are shown in Fig. 1. The dependences were determined at 700 °C for the electrodes made of different metals: Pt, Ag and Au located at the

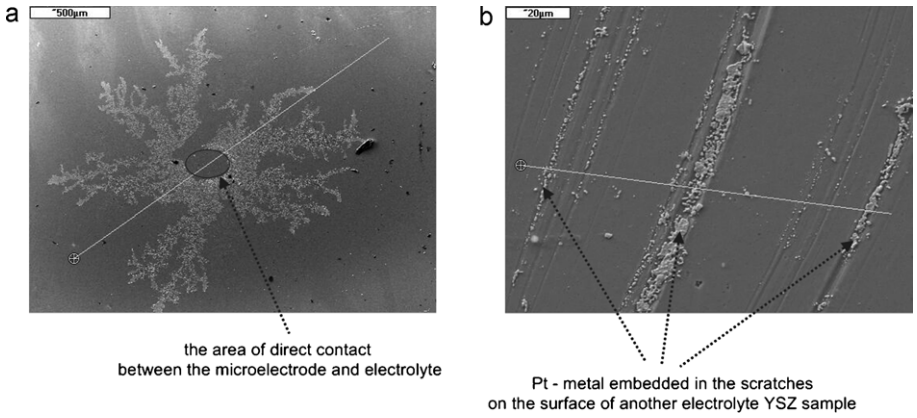

Fig. 2. SEM images of Pt contact area on the surface of 8YSZ electrolyte after polarization experiments (−0.5 V, 700 °C, in air): (a) the free space in the middle of the pictures resulted from ripping the electrode off; (b) Pt – metal embedded in the scratches at the surface of another sample of YSZ electrolyte.

20GDC electrolyte. The similar results were also obtained in the experiments carried out with the 8YSZ electrolyte; they were presented in paper [34]. Because the stable values of the currents were approached very slowly, especially at lower overpotentials, the experiments lasted at least 18 h. There are six curves presented for the each electrode in Fig. 1; the curves were recorded at overpotentials −0.05, −0.1, −0.15, −0.2, −0.25 and −0.3 V. Although the data in Fig. 1 are shown for an arbitrary chosen partial pressure of oxygen p_{O2} = 0.1 bar, the experiments were also carried out at p_{O2} = 0.01 and 1.0 bar.

The determined dependences of current vs. time for the step polarization show the following characteristics:

(a) Generally, within the overpotential range (−0.05 to −0.3 V), the absolute currents had a tendency to increase monotonically with the time for all the three electrode materials: Pt, Ag and Au and both electrolytes: 20GDC and 8YSZ.
(b) The increase of absolute current was more evident for the electrodes made of Pt and Ag than Au. As it can be seen in Fig. 1c, only for the Au electrode at overpotential −0.3 V, the absolute current decreased after the initial abrupt increase. This different character of the *i* vs. *t* dependence for the Au electrode may indicate that the processes occurring during the polarization of Au are different than during polarization of Pt and Ag.
(c) The character of dependences was qualitatively similar at all the investigated partial pressures of oxygen p_{O2} = 0.01, 0.1 and 1.0 bar.

We also carried out electrochemical impedance spectroscopy (EIS) measurements in the same conditions. The overall decrease of impedance was observed in duration of negative polarization which can be correlated with the behaviour of chronoaperometric curves in Fig. 1. The details of the EIS spectra analysis and other electrochemical research are described in our previous paper [35].

The SEM images of Pt and Ag electrode contact areas on the 8YSZ electrolyte after polarization experiments are shown in Figs. 2 and 3, respectively. The black hole in the middle of the SEM pictures corresponds to the area of direct contact between the microelectrode and electrolyte. Similar configurations of metal deposit were also observed on the 20GDC electrolyte. They are presented in Figs. 4 and 5. The EDS analysis confirmed that the structures shown in Figs. 2 and 4 and Figs. 3 and 5 consist mainly of metallic Pt and Ag, respectively. The XPS/ESCA analysis corroborated these results, though at the Ag|8YSZ interface, just under the electrode, the presence of AgO was also detected. The AFM inspections also showed the presence of Ag and Pt metallic particles, which appeared at the 8YSZ surfaces after the polarization of Ag and Pt electrodes respectively. The scans were performed partly within and partly outside the contact area. Inside the contact area a coarse structure, which will be referred to as a “hill and valley” structure, was formed. A ridge, higher than the surroundings, was seen at the borderline of the contact area. Outside of the contact area, the surface appeared smooth as compared to the “hill and valley” structure.

It can be clearly seen that the electrode is a source of migrated metal, which spreads around the electrode in a form of a dendrite-like structure. The increase of absolute currents observed at the chronoamperograms in Fig. 1 can be therefore explained, first of all, by the growth of a metallic zone around of the Pt and Ag electrodes.

The similar phenomenon was observed by Nielsen and Jacobson [25–27] for the Pt, Ag and Pd electrodes located at the 8YSZ electrolyte. Their experiments were carried out at much higher temperatures than ours, namely 920 °C for Ag and 1000 °C for other noble metals.

Although, quantitatively, the Pt and Ag dendrite structures looked similarly at both the electrolytes investigated, 8YSZ and 20GDC, the range and amount of migrated metal was always larger in the case of the latter electrolyte. In this way, the intensity of metal deposition in the vicinity of the electrode may indicate the importance of oxide ion conductivity, which is definitely higher in the 20GDC than 8YSZ. The patterns of migrated metals depend also on the material of electrode and smoothness of the electrolyte surface. Pt patterns are usually deposited in the form of a snowflake-like structure whereas Ag layer is more dense and forms a pretzel-like configuration. Any irregularity at the surface of the electrolyte (hollows, scratches, cracks and dislocations) interferes with the metal spreading and in consequence restricts growing of TPB length of the modified electrode. As it can be seen in Fig. 2b, the metal, which migrates from the electrode, has a tendency to agglomerate at the irregularities at the electrolyte surface. Therefore, the largest increase of the absolute current during the polarization of Pt or Ag electrode was observed for a mirror-like surface of electrolyte. When the electrolyte was only preliminarily polished with sandpaper, the absolute values of current responses were ca. three times lower than in the former case. The former phenomenon can be explained by a more developed and extended structure of metal deposit, whose growth is not hampered by scratches, cracks and scars at the mirror-like surface. This, in turn, results in the increase of TPB length of metal, where the oxygen electroreduction proceeds with the highest intensity. The effect of electrolyte surface smoothness on the response of the Ag electrode is shown in Fig. 6.

Contrary to the Pt and Ag electrode, no migration of metal into the vicinity of interface electrode|solid oxide electrolyte was observed for the Au electrodes. Therefore, the phenomenon

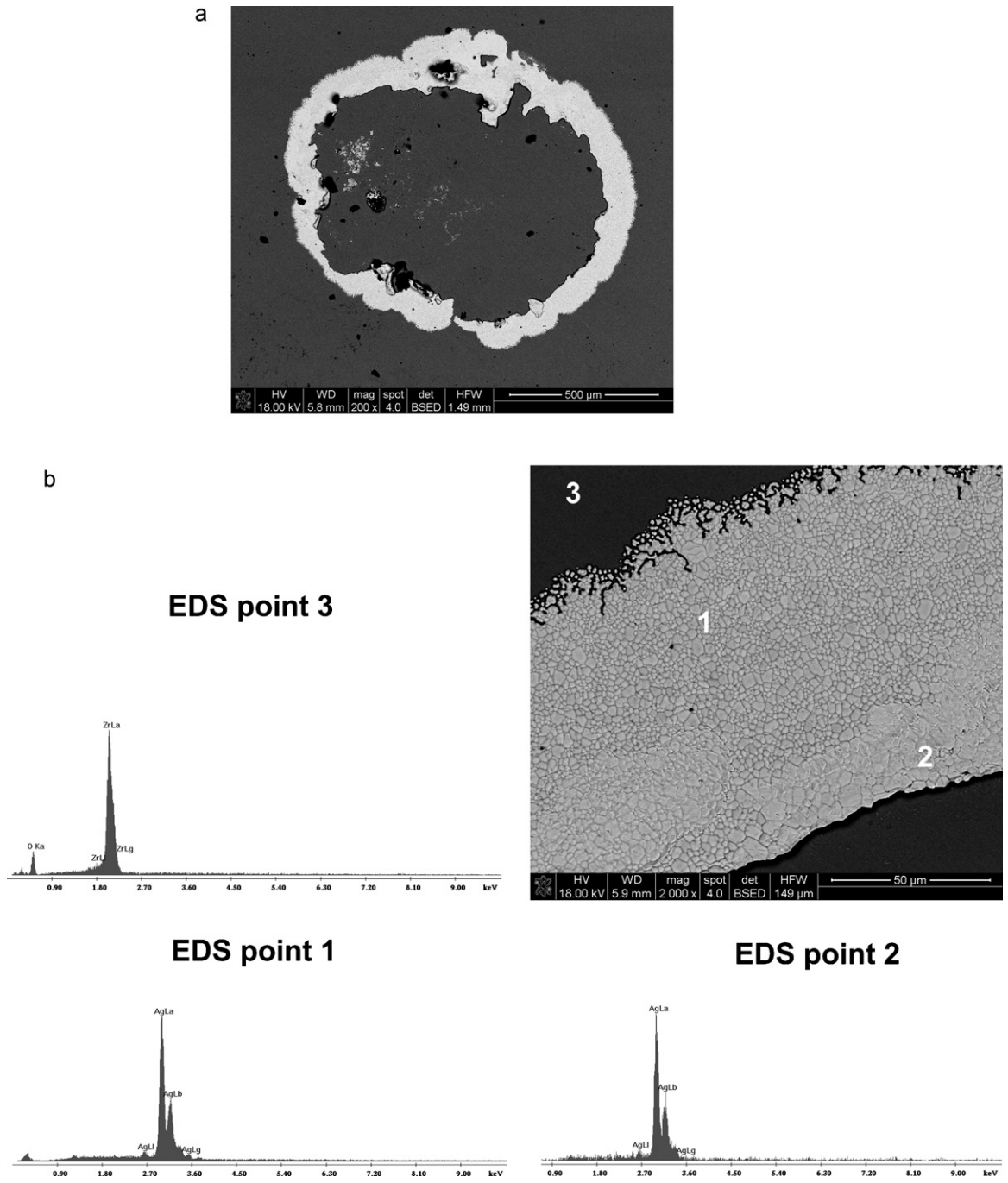

Fig. 3. SEM backscattered electron images of 8YSZ surface after polarization experiments (−0.5 V, 700 °C, in air): (a) Ag electrode contact area; (b) magnification of Ag deposit with EDS analysis.

reported in Fig. 1c cannot be explained by migration of gold, which results in the increase of the TPB length at the interface Au|8YSZ or 20GDC and consequent rise of absolute current with the polarization time. Nevertheless, after a very careful examination, the metallic gold was found at the surfaces of the both, 8YSZ and 20GDC, electrolytes but exclusively in the form of small Au dots, highly dispersed over the whole electrolyte area and located mostly in hollows and scratches at the surface (Fig. 7). Gold deposits were also observed in hollows at the electrolyte surface directly under the electrode.

Nielsen and Jacobsen were investigating the behaviour of Au|8YSZ interface during polarization at 1000 °C [26]. In this case, they did not report any Au migration from the electrode to the surface of electrolyte. However, the same authors pointed out in their next paper [27] that the Au|8YSZ interface exhibited a structure similar to the "hill and valley" structure reported for the Ni point electrodes; according to them the development of this structure was responsible for a nonstationary behaviour of the OER response at the Au electrodes.

To explain the mechanism of metal migration at the surface of the oxide electrolyte two more pieces of information should be taken into account:

(1) We investigated in separate experiments the phenomenon of Pt migration from the electrode located at the surface of solid state electrolyte with conducting ions other than O^{2-}:

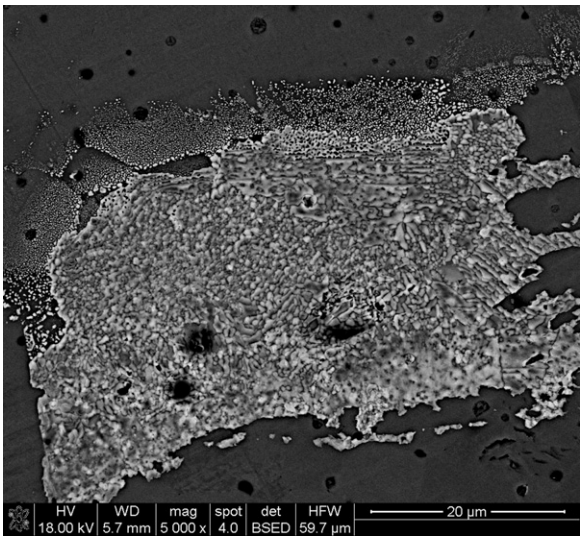

Fig. 4. SEM images of Pt deposit on the surface of 20GDC electrolyte after polarization experiments (−0.5 V, 700 °C, in air).

$BaZr_{0.9}Y_{0.1}O_3$ with dominant proton conductivity, CaF_2 with dominant F^- conductivity and LISICON with dominant Li^+ conductivity. Almost no migration of Pt at the surfaces of these electrolytes was observed in the vicinity of the polarized electrode. Hence, one may conclude that the presence of mobile O^{2-} ions in the electrolyte is necessary for the occurrence of Pt migration in the vicinity of the electrode.

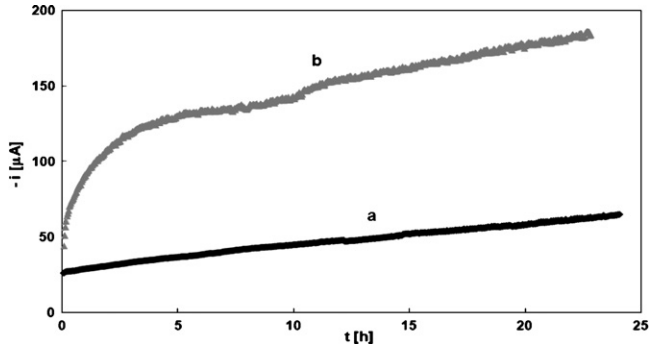

Fig. 6. Chronoamperometric curves (−0.5 V, 700 °C in air) recorded at the point Ag electrode in contact with 8YSZ electrolyte: (a) electrolyte surface preliminary polished with sandpaper, (b) electrolyte polished to the mirror-like surface.

(2) The equilibrium vapour pressures of Pt, Ag and Au and their selected oxides in an oxygen atmosphere at 700 °C are reported in Table 1. [36,37] On the basis of these data, the following sequence of these pressures over the metallic electrodes in the conditions of our experiments can be established in the range of 10^{-9}–10^{-13} atm:

$$p_{Ag}(3E^{-9}\ \text{atm}) > p_{PtO2}(5E^{-10}\ \text{atm}) > p_{AgO}(2E^{-11}\ \text{atm}) > p_{Au}(1E^{-13}\ \text{atm})$$

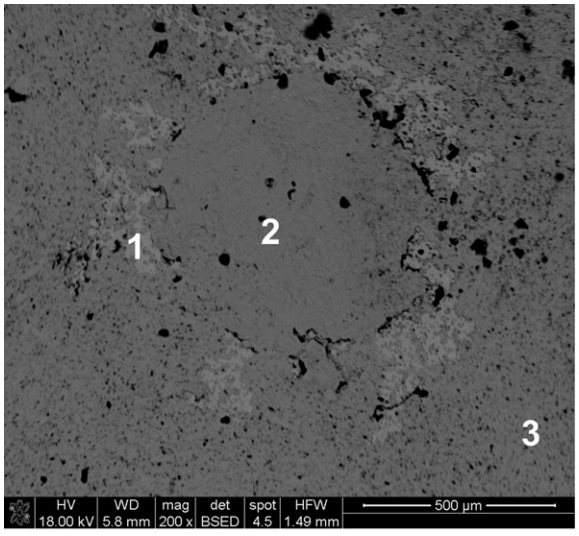

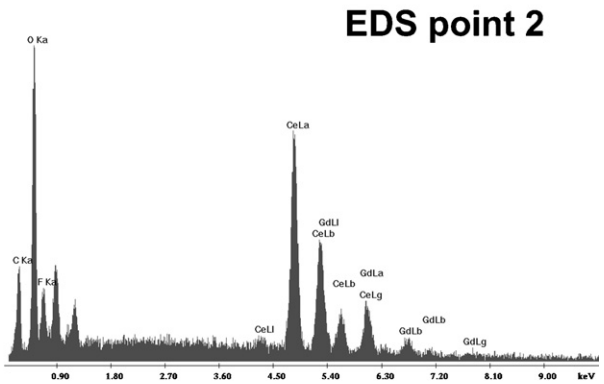

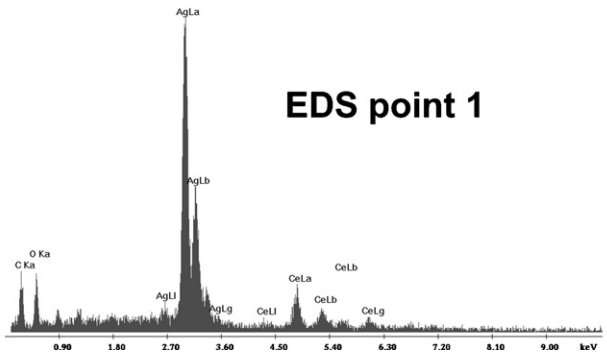

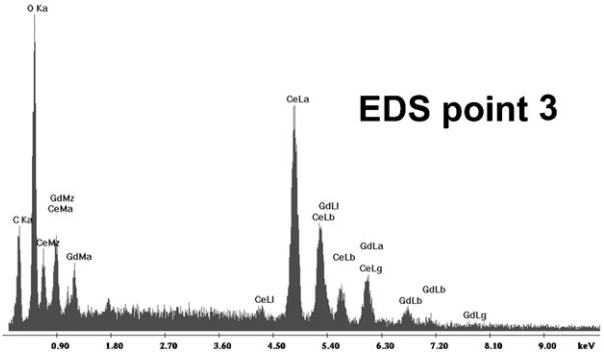

Fig. 5. SEM images of Ag contact area on the 20GDC electrolyte surface after polarization experiments (−0.5 V, 700 °C, in air). The results of EDS analysis in chosen points of the sample are also presented.

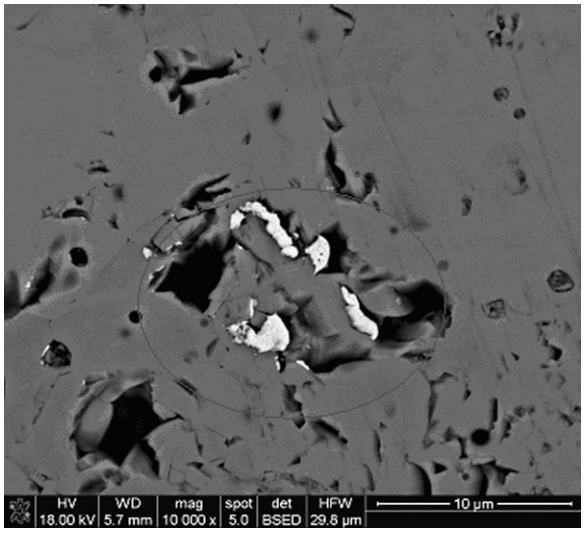

Fig. 7. SEM microphotograph of 20GDC surface after long-term polarization of Au|20GDC half cell (−0.5 V, 700 °C, in air). A circle marks the area of Au deposition.

That means that the deposition of the following species should dominate in the systems investigated: platinum oxides (but not metallic Pt), metallic silver and silver oxide and metallic Au (but not gold oxides). According to our observations, an extension of the metallic zone from the Pt electrode does not proceed without negative polarization of the electrode and participation of O^{2-} ions from the electrolyte (entry (1)). Since the deposit around of electrode consists mostly of pure metal in all cases investigated, one can conclude that platinum and silver oxides have to be reduced to metallic Pt and Ag during an electrochemical reaction, which occurs in the vicinity of the electrode. This reaction provides a progressive extension of Pt and Ag deposits in the form of a dendrite-like structure during polarization. Therefore, the following mechanism of Pt and Ag migration at the surface of oxide electrolyte can be proposed:

$$\mathrm{M(s)\ \ (electrode)} + n/2\mathrm{O_2} \rightarrow \mathrm{MO}_n\mathrm{(s)\ \ (electrode)} \quad (2)$$

$$\mathrm{MO}_n\mathrm{(s)\ \ (electrode)} \rightarrow \mathrm{MO}_n\mathrm{(g)} \quad (3)$$

$$\mathrm{MO}_n\mathrm{(g)} + 2ne^- \rightarrow \mathrm{M(s)} + n\mathrm{O}^{2-}$$

$$\mathrm{(at\ interface\ Pt\ and\ Ag|oxide\ electrolyte)} \quad (4)$$

In the case of Au electrode, gold deposits from a gaseous phase of metal and is not reduced in contact with the electrode. The sequence of reactions (5) and (6) justifies why the dendrite-like structure is not formed close to Au electrode. In these circumstances metal condensates, first of all, in irregularities of the electrolyte surface, which may be located even in a considerable distance from the electrode:

$$\mathrm{M(s)\ \ (electrode)} \rightarrow \mathrm{M(g)} \quad (5)$$

Table 1
Equilibrium vapour pressure (in 1 atm air, 700 °C) data of selected noble metal Ag, Au and Pt gaseous species over their respective solid elements [36,37].

Noble metal species	Partial pressure [atm]
Ag	$3E^{-9}$
AgO	$2E^{-11}$
Ag_2O	$6E^{-14}$
Pt	$4E^{-23}$
PtO	$5E^{-19}$
PtO_2	$5E^{-10}$
Au	$1E^{-13}$
AuO	$1E^{-16}$
Au_2O_3	$2E^{-19}$

$$\mathrm{M(g)} \rightarrow \mathrm{M(s)\ \ (Ag\ and\ Au\ dots\ at\ the\ whole\ surface\ of\ electrolyte)} \quad (6)$$

Recently, the increase of the absolute current flowing through the polarized Au electrode has been interpreted as a result of extension of the TPB length by channel formation along the electrode perimeter [27].

In the case of Ag, the deposition of the metallic structure around the electrode was observed to proceed faster than in the case of Pt – probably a coexistence of both mechanisms (2)–(4) and (5)–(6), together with relatively high pressure of Ag vapour, made this phenomenon more intensive.

However, also another explanation of Au electrode behaviour, based exclusively on the electrochemical elucidation of the processes, is theoretically permissible. The dependences presented in Fig. 1 are characteristic for a coupled catalytic reaction with quasi-reversible or reversible charge transfer [38]:

$$O + ne^- \rightarrow R \quad (7)$$

$$R + Z \rightarrow O + Y \quad (8)$$

where O and R represent oxidized and reduced entities, respectively, Z does not participate in electrode reaction (7) but reacts with a product of electroreduction. The following sequence of reactions may be proposed for the OER mechanism with a participation of superoxide ions (O_2^-):

$$\mathrm{O_2(g)} \rightarrow 2\mathrm{O_{ad}(electrode)} \quad (9)$$

$$\mathrm{O_{ad}} + 2e^- \rightarrow 2\mathrm{O}^{2-}\mathrm{(TPB)} \quad (10)$$

$$\mathrm{O}^{2-} + 3/2\mathrm{O_2} \rightarrow 2\mathrm{O_2}^-\mathrm{(electrolyte\ surface)} \quad (11)$$

$$\mathrm{O_2}^- + e^- \rightarrow 2\mathrm{O}^{2-} \quad (12)$$

A similar sequence can be also postulated for peroxide ions (O_2^{2-}). A formation of superoxide and peroxide ions at the surface of solid oxide electrolytes was suggested in numerous works, especially in the discussion of catalytic selective oxidation of some organic compound [39–42].

4. Conclusions

The mechanism of the oxygen electrode reaction in the solid oxide fuel cell is still not fully understood. Recently, a number of works have been carried out with microelectrodes to enlighten at least some of controversies over the OER. Unfortunately, the use of microelectrodes appeared to be only a little helpful for clarifying the controversies but it revealed also a new unresolved issue, namely the so called, nonstationary behaviour of metallic electrodes, such as a distinct increase of the absolute current flowing through the electrode located on solid oxide electrolyte during the prolonged negative polarization. Such an unusual behaviour was explained by the increase of the three-phase boundary length due to deposition and subsequent reduction of metal oxides around the Pt and Ag electrodes. However, in the case of the Au electrode, no pattern of migrated metal was observed in the vicinity of the electrode. In this case, an occurrence of autocatalytic electrode reaction was suggested to explain the phenomenon.

Acknowledgement

This work was sponsored by the MNiSzW grant no. N N209 145336.

References

[1] K. Huang, J.B. Goodenough, Solid Oxide Fuel Cell Technology: Principles, Performance and Operations, Woodhead Publishing Limited, Cambridge, 2010.
[2] S.B. Adler, Chem. Rev. 104 (2004) 4791–4843.
[3] Y. Li, R. Gemmen, X. Liu, J. Power Sources 195 (2010) 3345–3358.
[4] J.S. Newman, Electrochemical Systems, 2nd ed., Prentice Hall, New York, 1991.
[5] D.Y. Wang, A.S. Nowick, J. Electrochem. Soc. 126 (1979) 1166–1172.
[6] D.Y. Wang, A.S. Nowick, J. Electrochem. Soc. 126 (1979) 1155–1165.
[7] H. Okamoto, G. Kawamura, T. Kudo, Electrochim. Acta 28 (1983) 379–382.
[8] H. Hu, M. Liu, J. Electrochem. Soc. 144 (1997) 3561–3567.
[9] A.J. Bard, L.R. Faulkner, Electrochemical Methods, 2nd ed., John Wiley and Sons, 2001.
[10] E. Schouler, G. Giroud, M. Kleitz, J. Chim. Phys. Phys. Chim. Biol. 70 (1973) 1309–1316.
[11] E. Barsoukov, J. Ross Macdonald, Impedance Spectroscopy: Theory, Experiment, and Applications, 2nd ed., John Wiley & Sons, Inc., 2005.
[12] Q.-A. Huanga, R. Huia, B. Wang, J. Zhang, Electrochim. Acta 52 (2007) 8144–8164.
[13] J. Mizusaki, K. Amano, S. Yamauchi, K. Fueki, Solid State Ionics 22 (1987) 313–322.
[14] J. Mizusaki, K. Amano, S. Yamauchi, K. Fueki, Solid State Ionics 22 (1987) 323–330.
[15] D.Y. Wang, J. Electrochem. Soc. 137 (1990) 3660–3666.
[16] B.A. van Hassel, B.A. Boukamp, A.J. Burggraaf, Solid State Ionics 48 (1991) 139–154.
[17] N.L. Robertson, J.N. Michaels, J. Electrochem. Soc. 137 (1990) 129–135.
[18] A. Mitterdorfer, L. Gauckler, Solid State Ionics 117 (1999) 187–202.
[19] A. Mitterdorfer, L. Gauckler, Solid State Ionics 117 (1999) 203–217.
[20] A. Mitterdorfer, L. Gauckler, Solid State Ionics 120 (1999) 211–225.
[21] L. Bay, T. Jacobsen, Solid State Ionics 93 (1997) 201–206.
[22] B. Zachau-Christiansen, T. Jacobsen, L. Bay, S. Skaarup, Silid State Ionics 113–115 (1998) 271–277.
[23] T. Jacobsen, B. Zachau-Christiansen, L. Bay, M. Juhl Jørgensen, Electrochim. Acta 46 (2001) 1019–1024.
[24] T. Jacobsen, L. Bay, Electrochim. Acta 47 (2002) 2177–2181.
[25] J. Nielsen, T. Jacobsen, Solid State Ionics 178 (2007) 1001–1009.
[26] J. Nielsen, T. Jacobsen, Solid State Ionics 178 (2008) 1769–1776.
[27] J. Nielsen, T. Jacobsen, Solid State Ionics 179 (2008) 1314–1319.
[28] E. Ivers-Tiffée, A. Weber, K. Schmid, V. Krebs, Solid State Ionics 174 (2004) 223–232.
[29] S.P. Jiang, J.G. Love, Solid State Ionics 138 (2001) 183–190.
[30] F.S. Baumann, J. Fleig, M. Konuma, U. Starke, H.-U. Habermeier, J. Maier, J. Electrochem. Soc. 152 (2005) A2074.
[31] X.J. Chen, K.A. Khor, S.H. Chan, Solid State Ionics 167 (2004) 379–387.
[32] S.P. Jiang, J. Power Sources 124 (2003) 390–402.
[33] W. Wang, S.P. Jiang, ECS Trans. 7 (1) (2007) 875–876.
[34] P. Tomczyk, S. Żurek, M. Mosiałek, J. Electroceram. 23 (2009) 25–36.
[35] A. Raźniak, P. Tomczyk, Mater. Sci.-Poland 26 (2008) 196–206.
[36] S.P. Simner, M.D. Anderson, L.R. Peterson, J.W. Stevenson, J. Electrochem. Soc. 152 (2005) A1851–A1859.
[37] O. Knacke, O. Kubaschewski, K. Hessemann (Eds.), Thermochemical Properties of Inorganic Substances, 2nd ed., Springer, Berlin, 1991.
[38] A.J. Bard, L.R. Faulkner, Electrochemical Methods Fundamentals and Applications, John Wiley & Sons, New York, 1980, p. 431.
[39] A. Bielański, J. Haber, Oxygen in Catalysis, Marcel Dekker, Inc., N.Y., 1991.
[40] C. Descorme, Y. Madier, D. Duprez, J. Catal. 196 (2000) 167–173.
[41] K. Otsuka, T. Ando, S. Suprapto, Y. Wang, K. Ebitani, I. Yamanaka, Catal. Today 24 (1995) 315–320.
[42] V.V. Pushkarev, V.J. Kovalchuck, J.L. d'Itri, J. Phys. Chem. B 108 (2004) 5341–5348.